

NMR $^{\text{h}^3}J_{\text{NC}}$ Couplings Provide Comprehensive Geometrical Constraints for Protein H-bonds in Solution*

Nenad Juranić,^{a,**} Martin C. Moncrieffe,^c Elena Atanasova,^b Slobodan Macura,^a
and Franklyn G. Prendergast^{a,b}

^aDepartment of Biochemistry and Molecular Biology, Mayo College of Medicine,
Mayo Clinic and Foundation, Rochester, Minnesota, 55905 USA

^bDepartment of Molecular Pharmacology and Experimental Therapeutics, Mayo College of Medicine,
Mayo Clinic and Foundation, Rochester, Minnesota, 55905 USA

^cDepartment of Biochemistry, University of Cambridge, Cambridge, CB2 JGA, UK

RECEIVED SEPTEMBER 28, 2005; REVISED FEBRUARY 15, 2006; ACCEPTED MARCH 16, 2006

Keywords
hydrogen bonding
proteins
NMR
spin-spin couplings
H-bond geometry

Protein backbone H-bonds ($>\text{N}-\text{H}\cdots\text{O}-\text{C}<$) show relationships between NMR $^{\text{h}^3}J_{\text{NC}}$ couplings measured in solution and H-bond geometry parameters seen in X-ray crystal structures. Assuming that the solution and crystal structure of protein backbone is the same, the $^{\text{h}^3}J_{\text{NC}}$ couplings can be calibrated to provide good estimates of both angular and radial H-bond parameters in a solution. The crucial premise of equality between the solution and the crystal structure of protein backbone we validated on the level of the NH-bonds orientation, by comparing the orientations inferred from X-ray crystal structures with the solution ones determined from NMR residual dipolar couplings.

INTRODUCTION

The most detailed data concerning hydrogen bonds (H-bonds) in proteins have been obtained from the high-resolution X-ray crystal structures.¹ In X-ray crystallography, the position of heavy atoms is the principal source of information and, consequently, the presence of H-bonds is inferred from the local geometry. The detection of $^{\text{h}^3}J_{\text{NC}}$ coupling across the backbone H-bonds ($>\text{NH}\cdots\text{OC}<$) in proteins^{2,3} has provided a major advance in that H-bonds can now be detected experimentally by identifying the donor-acceptor pairs, without prior knowledge of the structure. Consequently, H-bonds identified in this man-

ner can be used to verify the structure of proteins in solution. The H-bond distance could be predicted from $^{\text{h}^3}J_{\text{NC}}$ couplings^{4,5} with precision of approximately 0.1 Å, which has been used for a refinement of the NMR derived protein structures.⁶ The experimental detection of H-bonds was followed by theoretical analyses that formulated the $^{\text{h}^3}J_{\text{NC}}$ dependence on the H-bond geometry.^{5,7} Beside the preponderant dependence on the H-bond distance, the theory⁵ predicts strong dependence on angular parameters at the acceptor (α_{O} , Scheme 1), with no dependence on the donor angle (α_{H}). This suggests that $^{\text{h}^3}J_{\text{NC}}$ couplings would not provide effective constraint for refinement of the angular part of H-bond geometry in solution,

* Communicated in part at MATH/CHEM/COMP 2005, Dubrovnik, Croatia, June 20–25, 2005.

** Author to whom correspondence should be addressed. (E-mail: juranic.nenad@mayo.edu)

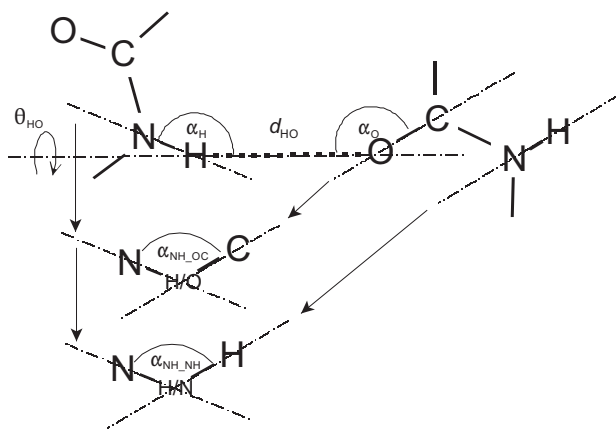
because of the insensitivity to the H-bond donor parameters.

In this work we analyze experimental data from four proteins (≈ 200 $^3J_{\text{NC}}$ values) and show relationships between $^3J_{\text{NC}}$ couplings and parameters related to H-bond geometry inferred from X-ray crystal structures of the same proteins. The proteins range from the α -helical (parvalbumin and calmodulin) to a fused α/β ubiquitin to the β -barrel fatty acid binding protein.

RESULTS AND DISCUSSION

The major obstacle in the analysis of the $^3J_{\text{NC}}$ coupling dependence on H-bond geometry is the un-availability of detailed information on that geometry in solution. Therefore, the analyses have been relying on the heavy-atom H-bond geometry seen in the X-ray crystal structures of proteins. Since $^3J_{\text{NC}}$ couplings depend on the H-atom position in the H-bonds, hydrogen atoms have to be added to X-ray determined protein structures. For the four proteins studied here, human ubiquitin (1ubq),⁸ carp parvalbumin (4cpv),⁹ rat intestinal fatty acid binding protein (1ifc),¹⁰ and calmodulin (1cll)¹¹ we added amide protons in the respective PDB structures at their ideal positions using CHARMm software, and set NH distance to 1.01 Å, the value seen experimentally in the ultra high-resolution structure of crambin of (1ejg.pdb).¹²

To validate the relevance of so obtained H-bond geometry in solution, we compared orientations of the N–H bonds from X-ray models with those determined from NMR structures optimized by the method of residual dipolar couplings (RDC).^{13,14} In doing so we recognized that the angular property of the H-bond could be characterized by an angle of non-collinearity between the N–H and O–C bonds. The non-collinearity angle (equal to zero for co-linear bonds) can be related to a putative bond angle



Scheme 1. Parameters of the H-bond geometry used in this work: distance (d_{HO}), bond angle N–H...O (α_{H}), bond angle H...O=C (α_{O}) and dihedral angle N–H...O=C (θ_{HO}). Straight arrows indicate translations of NH and OC bonds needed to construct the putative bond angles N–H/O–C ($\alpha_{\text{NH}_{\text{OC}}}$) and N–H/N–H ($\alpha_{\text{NH}_{\text{NH}}}$).

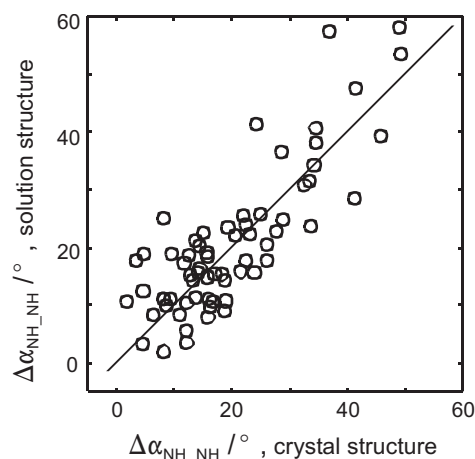


Figure 1. Comparison of non-collinearity of NH vectors in the H-bonded peptide groups ($\Delta\alpha_{\text{NH}_{\text{NH}}}$) from the X-ray crystal structures with those from the RDC-optimized NMR solution structures. The corresponding structures are ubiquitin (1ubq versus 1d3z)⁶ and calmodulin (1cll versus 1j7o & 1j7p)¹⁷.

between the two bonds ($\alpha_{\text{NH}_{\text{OC}}}$, Scheme 1) by defining it as: $\Delta\alpha_{\text{NH}_{\text{OC}}} = 180 - \alpha_{\text{NH}_{\text{OC}}}$.

The angle of non-collinearity is invariant to translations of peptide groups, unlike other H-bond geometry parameters, and could be determined experimentally for proteins in solution by the RDCs of the peptide groups. One can not determine orientation of the OC bonds directly because oxygen does not have nucleus with the necessary NMR properties. However, due to peptide group geometry (Scheme 1), the non-collinearity of N–H bond vectors ($\Delta\alpha_{\text{NH}_{\text{NH}}}$) is equal to within few degrees to $\Delta\alpha_{\text{NH}_{\text{OC}}}$. Therefore, we can compare $\alpha_{\text{NH}_{\text{NH}}}$ from the X-ray crystal structure with $\Delta\alpha_{\text{NH}_{\text{NH}}}$ from RDC optimized NMR solution structures, as presented in Figure 1.

The solution values agree with the solid-state values with standard deviation of about 8 degrees. The agreement signifies that solid state H-bond geometry is a reasonably good approximation for the solution H-bond geometry, considering increased H-bond dynamics of protein in solution.^{15,16}

Dependence of $^3J_{\text{NC}}$ couplings on H-bond geometry can now be assessed upon assumption that X-ray crystal-structure data are relevant for proteins in solution. By this approach we can show that both the acceptor (α_{O}) and donor angle (α_{H}) get confined more closely to the value of linear H-bond with the increase of $^3J_{\text{NC}}$ couplings. To keep in line with the introduced angle of non-collinearity we have presented H-bond angles in terms of the angles of non-linearity ($\Delta\alpha = 180 - \alpha$, Figure 2a,b). The confinement boundary for the acceptor angle (Figure 2a) is depicted using the theoretical dependence ($-^3J_{\text{NC}} \approx \cos^2\alpha_{\text{O}}$)⁵, while for other angles (where theory does not predict dependence) we used linear boundary (Figure 2b). Interestingly, the $\Delta\alpha_{\text{NH}_{\text{NH}}}$ angle shows that collinearity is a more conserved property for the $^3J_{\text{NC}}$

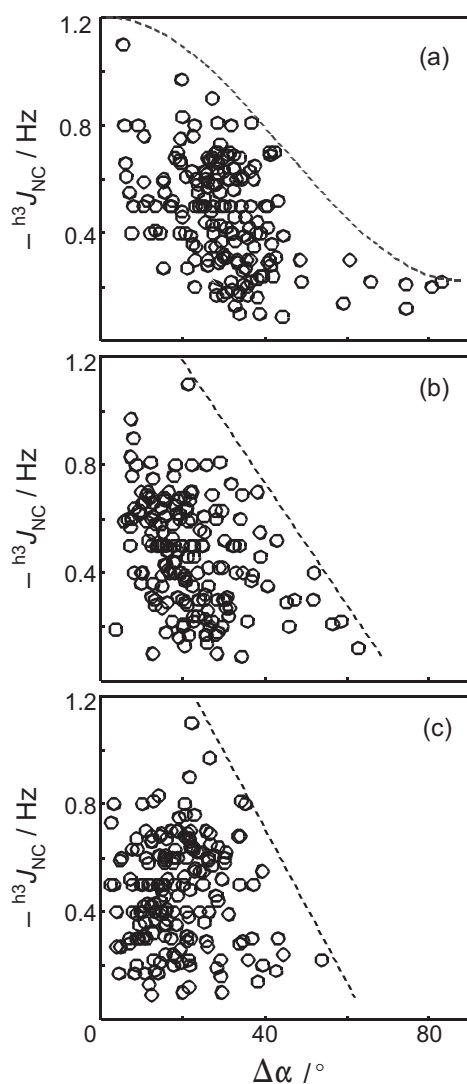


Figure 2. Dependence of ${}^{\text{h}3}\text{J}_{\text{NC}}$ couplings on: (a) non-linearity of $\text{H}\cdots\text{O}=\text{C}$ angle ($\Delta\alpha_{\text{O}}$); (b) non-linearity of $\text{N}-\text{H}\cdots\text{O}$ angle ($\Delta\alpha_{\text{H}}$); (c) non-collinearity of $\text{N}-\text{H}$ and $\text{O}=\text{C}$ bonds ($\Delta\alpha_{\text{NH}_{\text{OC}}}$, $\Delta\alpha_{\text{NH}_{\text{NH}}}$). Dashed lines represent the approximate boundary of the confinement of the non-linearity/collinearity angles. The ${}^{\text{h}3}\text{J}_{\text{NC}}$ couplings for three proteins (ubiquitin, carp-parvalbumin and intestinal fatty acid protein) are from our earlier work¹⁸ and data for calmodulin are new (Supporting Information). The angles of non-linearity ($\Delta\alpha_{\text{O}}$, $\Delta\alpha_{\text{H}}$) and angle of non-collinearity ($\Delta\alpha_{\text{NH}_{\text{OC}}}$) are from the crystal-structure PDBs of ubiquitin (1ubq), carp-parvalbumin (4cpv), intestinal fatty-acid binding protein (1ifc) and calmodulin (1cll).

detected H-bonds than linearity (Figure 2c), *i.e.* $\Delta\alpha_{\text{NH}_{\text{OC}}}$ is generally smaller than $\Delta\alpha_{\text{O}}$ or $\Delta\alpha_{\text{H}}$. Such result is consequence (see Eq. 1) of the nature of protein secondary structure in which the H-bonded peptide groups rarely have dihedral angle $|\theta_{\text{HO}}|$ less than 90° (for here considered set of H-bonds $|\theta_{\text{HO}}|$ averages to $145^\circ \pm 35^\circ$).

$$\Delta\alpha_{\text{NH}_{\text{OC}}} =$$

$$\arccos \{ (\cos [\Delta\alpha_{\text{H}} + \arctan (\tan \Delta\alpha_{\text{O}} \cos \theta_{\text{HO}})]) \sqrt{\cos^2 \Delta\alpha_{\text{O}} + \sin^2 \Delta\alpha_{\text{O}} \cos^2 \theta_{\text{HO}}} \}, (\Delta\alpha_{\text{O}} < 90^\circ) \quad (1)$$

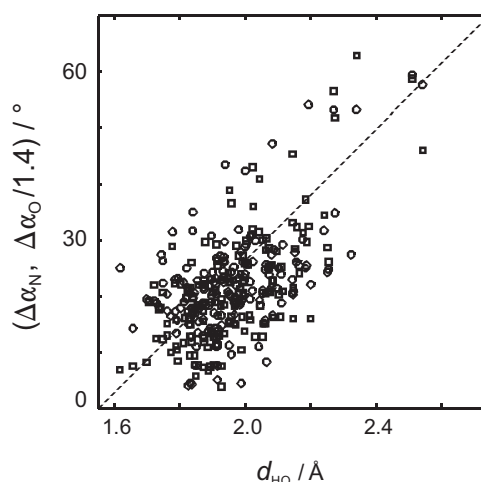


Figure 3. Inter-dependence of H-bond geometrical parameters: (O) $\Delta\alpha_{\text{O}}/1.4$ vs. d_{HO} and (□) $\Delta\alpha_{\text{H}}$ vs. d_{HO} .

Furthermore, $\Delta\alpha_{\text{O}}$ or $\Delta\alpha_{\text{H}}$ are correlated to each other ($|\Delta\alpha_{\text{O}} - \Delta\alpha_{\text{H}}| \approx 12^\circ \pm 8^\circ$), as well as to H-bond distance, which is presented in Figure 3. To assess impact of the correlation between H-bond angles we can simplify Eq. (1) by setting $\theta_{\text{HO}} = 180^\circ$, which gives:

$$\Delta\alpha_{\text{NH}_{\text{OC}}} = |\Delta\alpha_{\text{H}} - \Delta\alpha_{\text{O}}| \quad 12^\circ \pm 8^\circ \quad (2)$$

Taking into account that $|\theta_{\text{HO}}| \approx 145^\circ$, we expect that $\Delta\alpha_{\text{NH}_{\text{OC}}}$ vary around 20° , which is indeed observed (histogram shown in the »graphic content entry« of this paper). Accordingly, for the H-bonds having $|\text{h}^3\text{J}_{\text{NC}}| > 0.3$ Hz, we can state:

$$\Delta\alpha_{\text{NH}_{\text{NH}}} = 20^\circ \pm 10^\circ \quad (3)$$

Such a strong confinement of collinearity provides an excellent angular constraint for the H-bonds detected by the ${}^{\text{h}3}\text{J}_{\text{NC}}$ couplings. Theoretical analysis of the ${}^{\text{h}3}\text{J}_{\text{NC}}$ couplings dependence on H-bond geometry has not indicated this finding because the spin-spin coupling mechanism appears insensitive to H-bond donor geometry.

The H-bond distance has preponderant influence on the ${}^{\text{h}3}\text{J}_{\text{NC}}$ couplings,⁴ which allows distance constraints to be evaluated directly from the couplings. By theory, the ${}^{\text{h}3}\text{J}_{\text{NC}}$ couplings depend exponentially on H-bond distance,⁵ which indeed is indicated by data presented in Figure 4. It allows estimate of the H-bond distance as:

$$d_{\text{HO}} = 1.65 - 0.3 \log (-\text{h}^3\text{J}_{\text{NC}}) \pm 0.12 \text{ \AA} \quad (4)$$

This H-bond d_{HO} distance calibration is similar to previous one for d_{NO} .

Additional constraints of the angular part of H-bond geometry, that will include approximate confinements depicted in Figure 2a,b can be derived either directly from the ${}^{\text{h}3}\text{J}_{\text{NC}}$ couplings or indirectly via dependence of

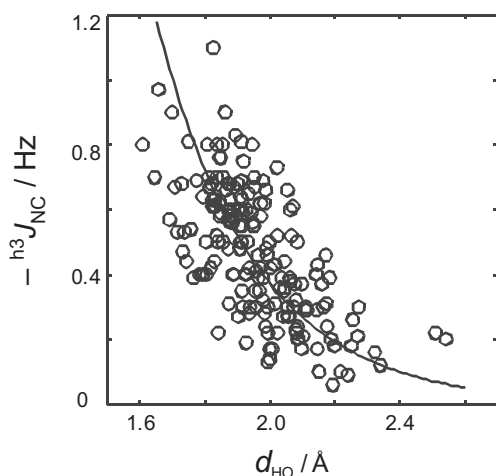


Figure 4. Dependence of ${}^{\text{h}^3}\text{J}_{\text{NC}}$ couplings on the H-bond distance (d_{HO}). The solid line represents the equation: $-{}^{\text{h}^3}\text{J}_{\text{NC}} = \exp[-3.3(d_{\text{HO}} - 1.70)]$.

$\Delta\alpha_{\text{O}}$ or $\Delta\alpha_{\text{H}}$ on the H-bond distance (Figure 3). We found that indirect path gives significantly better correlation between the angles and the couplings. As shown in Figure 3, we can approximate $\Delta\alpha_{\text{N}} \sim \Delta\alpha_{\text{O}}/1.4 \sim \frac{180}{\pi}(d_{\text{HO}}/\text{Å} - 1.55)$, therefore we can formulate the constraints as:

$$\begin{aligned} \Delta\alpha_{\text{O}} &= \frac{180^\circ}{\pi} \{0.1 - 0.3 \log[-{}^{\text{h}^3}\text{J}_{\text{NC}}/\text{Hz}]\} 1.4 \pm 12^\circ \\ \Delta\alpha_{\text{H}} &= \frac{180^\circ}{\pi} \{0.1 - 0.3 \log[-{}^{\text{h}^3}\text{J}_{\text{NC}}/\text{Hz}]\} \pm 12^\circ \end{aligned} \quad (5)$$

Finally, we should stress that analysis in terms of multi-parameter dependence of the ${}^{\text{h}^3}\text{J}_{\text{NC}}$ couplings on H-bond geometry, has been subject of several works.^{5,7,11} While such dependences provide good estimate of the ${}^{\text{h}^3}\text{J}_{\text{NC}}$ couplings from H-bond geometry, they are not suitable for the estimates in the opposite direction. For instance, the two parameter term $\cos^2\alpha_{\text{O}} \exp[-3.2(d_{\text{HO}} - d_0)]$, the most important term according to the theory,⁵ allows existence of a very short and non-linear H-bonds. However, such combination of parameters is not supported by the constraints presented here.

CONCLUSION

The spin-spin coupling mechanism that gives rise to ${}^{\text{h}^3}\text{J}_{\text{NC}}$ coupling across the protein backbone H-bond appears insensitive to H-bond geometry at the donor site. However, a broader environment of peptide groups within protein secondary structure imposes correlations between H-bond parameters. For instance, the short H-bonds tend to be more linear at the donor site,¹⁹ and consequently, the large ${}^{\text{h}^3}\text{J}_{\text{NC}}$ couplings have to be associated with linear H-bonds.

The ${}^{\text{h}^3}\text{J}_{\text{NC}}$ couplings detected in solution provide good estimates of H-bond angular ($\Delta\alpha_{\text{NH}_{\text{OC}}}$, $\Delta\alpha_{\text{O}}$, $\Delta\alpha_{\text{H}}$) and radial (d_{HO}) parameters. Their inclusion as restraints should improve NMR-derived protein structures. That result is especially important for protein structure determination by RDC,^{13,14} because it can be used for construction of an initial substructure (an element of protein secondary structure rich in the backbone H-bonds) that will afford proper resolution of the protein alignment tensor using a single orientation media.

Supporting Information Available. Table of ${}^{\text{h}^3}\text{J}_{\text{NC}}$ couplings for Ca^{2+} -calmodulin with experimental details.

REFERENCES

1. E. N. Baker and R. E. Hubbard, *Prog. Biophys. Mol. Biol.* **44** (1984) 97–179.
2. E. Cordier and S. Grzesiek, *J. Am. Chem. Soc.* **121** (1999) 1601–1602.
3. G. Cornilescu, J. S. Hu, and A. Bax, *J. Am. Chem. Soc.* **121** (1999) 2949–2950.
4. G. Cornilescu, B. E. Ramirez, M. K. Frank, G. M. Clore, A. M. Gronenborn, and A. Bax, *J. Am. Chem. Soc.* **121** (1999) 6275–6279.
5. M. Barfield, *J. Am. Chem. Soc.* **124** (2002) 4158–4168.
6. G. Cornilescu, J. L. Marquardt, M. Ottiger, and A. Bax, *J. Am. Chem. Soc.* **120** (1998) 6836–6837.
7. A. Bagno, *Chem. Eur. J.* **6** (2000) 2925–2930.
8. S. Vijay-Kumar, C. E. Bugg, and W. J. Cook, *J. Mol. Biol.* **194** (1987) 531–544.
9. V. D. Kumar, L. Lee, and B. F. Edwards, *Biochemistry* **29** (1990) 1404–1412.
10. G. Scapin, J. I. Gordon, and J. C. Sacchettini, *J. Biol. Chem.* **267** (1992) 4253–4269.
11. R. Chattopadhyaya, W. E. Meador, A. R. Means, and F. A. Quiocho, *J. Mol. Biol.* **228** (1992) 1177–1192.
12. G. A. Jeffrey, J. R. Ruble, R. K. McMullan, D. J. DeFrees, J. S. Binkley, and J. A. Pople, *Acta Crystallogr., Sect. B* **36** (1980) 2292–2299.
13. A. Bax, J. J. Chou, and B. E. Ramirez, in: D. M. Grant and R. K. Harris (Eds.), *Encyclopedia of Nuclear Magnetic Resonance*, Vol. 9, John-Wiley & Sons, New York, 1966, pp. 401–412.
14. R. A. Venters, R. Thompson, and J. Cavanagh, *J. Mol. Struct.* **602** (2002) 275–292.
15. M. Buck and M. Karplus, *J. Phys. Chem. B* **105** (2001) 11000–11015.
16. P. R. L. Markwick, R. Sprangers, and M. C. F. Sattler, *J. Am. Chem. Soc.* **125** (2003) 6337–6337.
17. J. J. Chou, S. P. Li, C. B. Klee, and A. Bax, *Nature Struct. Biol.* **8** (2001) 990–997.
18. N. Juranić, M. C. Moncrieffe, V. A. Likic, F. G. Prendergast, and S. Macura, *J. Am. Chem. Soc.* **124** (2002) 14221–14226.
19. R. S. Lipsitz, Y. Sharma, B. R. Brooks and N. Tjandra, *J. Am. Chem. Soc.* **124** (2002) 10621–10626.

SAŽETAK

$^3J_{NC}$ NMR sprege daju geometrijske uvjete za vodikove veze proteina u otopinama

Nenad Juranić, Martin C. Moncrieffe, Elena Atanasova, Slobodan Macura i Franklyn G. Prendergast

Prikazana je korelacija između $^3J_{NC}$ NMR sprege izmjerenih u otopini i geometrijskih parametara vodikovih veza ($>N-H\cdots O-C<$) glavnog proteinskog lanca u kristalnoj strukturi. Uz pretpostavku da su geometrije proteinskih lanaca u otopini jednake onima u kristalnim strukturama, moguće je kalibrirati $^3J_{NC}$ sprege za procjenu kutova i duljina vodikovih veza u otopinama. Bitna pretpostavka o očuvanju geometrije proteinskog lanca iz kristalne strukture u otopini potvrđena je usporedbom orijentacija N-H veza iz kristalne strukture s onima u otopini, određenima iz rezidualnih dipolarnih NMR sprege.